S100A1 Utilizes Different Mechanisms for Interacting with Calcium-Dependent and Calcium-Independent Target Proteins †

ARTICLE *in* BIOCHEMISTRY · JANUARY 1999

Impact Factor: 3.02 · DOI: 10.1021/bi9817921 · Source: PubMed

S100A1 Utilizes Different Mechanisms for Interacting with Calcium-Dependent and Calcium-Independent Target Proteins†

Aimee Landar,‡ Richard R. Rustandi,§ David J. Weber,§ and Danna B. Zimmer*,‡

Department of Pharmacology, MSB 3130, College of Medicine, University of South Alabama, Mobile, Alabama 36688, and the Department of Biological Chemistry, University of Maryland School of Medicine, Baltimore, Maryland 21201

Received July 24, 1998; Revised Manuscript Received October 6, 1998

ABSTRACT: While previous studies have identified target proteins that interact with S100A1 in a calcium-dependent manner as well as target proteins that interact in a calcium-independent manner, the molecular mechanisms of S100A1−target protein interaction have not been elucidated. In this study, point and deletion mutants of S100A1 were used to investigate the contribution of carboxyl terminal amino acids to S100A1 interaction with calcium-dependent and calcium-independent target proteins. First, a recombinant rat S100A1 protein (recS100A1) expressed in bacteria exhibited physical and chemical properties indistinguishable from native S100A1. Next, proteins lacking the carboxyl-terminal nine residues of recS100A1 (Δ85−93), or containing alanine substitutions at Phe 88 (F88A), Phe 89 (F89A), or Trp 90 (W90A), both Phe 88 and Phe 89 (F88/89A), or all three aromatic residues (F88/89A−W90A) were recombinantly expressed. Like recS100A1, F88A, F89A, and W90A proteins interacted with phenyl-Sepharose in a calcium-dependent manner. However, the Δ85−93 protein did not interact with phenyl-Sepharose, indicating that a phenyl-Sepharose-binding region (PSBR) of recS100A1 had been disrupted. The F88/89A and F88/89A−W90A proteins exhibited reduced calcium-dependent interaction with phenyl-Sepharose when compared with recS100A1, demonstrating that the carboxyl-terminal aromatic residues Phe 88, Phe 89, and Trp 90 comprise the PSBR of S100A1. Fluorescence studies showed that the Δ85−93 protein exhibited reduced calcium-dependent interaction with the dodecyl CapZ peptide, TRTK, while W90A bound TRTK with a K_d of 5.55 μM. These results demonstrate that the calcium-dependent target protein-binding site and the PSBR are indistinguishable. In contrast to the calcium-dependent target TRTK, activation of the calcium-independent target protein aldolase A by the point and deletion mutant S100A1s was indistinguishable from native S100A1. These results demonstrate that carboxyl-terminal residues are not required for S100A1 modulation of calcium-independent target protein aldolase A. Alltogether, these results indicate that S100A1 utilizes distinct mechanisms for interaction with calcium-independent and calcium-dependent target proteins.

The S100 protein family is a group of acidic, low molecular mass EF-hand calcium-receptor proteins which share approximately 50% amino acid sequence similarity (see ref *1*). Calcium receptor proteins, like the S100 proteins, have no known enzymatic activity and regulate cellular processes by interacting with and modulating the function of other proteins, termed "target proteins". The first members of the S100 protein family, S100α and S100*β*, were originally isolated as a brain-specific protein fraction which was partially soluble in 100% saturated ammonium sulfate, hence the name "S100" (*2*). There are currently 18 members of the S100 protein family. The genes for 13 S100 proteins are found in a cluster on the q21 region of chromosome 1 in humans. Genes for other members of the family are dispersed throughout the genome on other chromosomes. A nomenclature which reflects this genomic organization (*3*) has been recently adopted and is used throughout this manuscript: S100α is now designated S100A1 and S100*β* is designated S100B.

Analysis of intact cells in which the expression of S100 proteins has been ablated or upregulated have provided important insights into the cellular processes which are regulated by the various members of this family as well as their potential role in disease processes. Ablation of S100A1 expression in PC12 cells results in increased tubulin levels, altered neurite organization, and decreased cell proliferation (*4*). Interestingly, these phenotypic effects occurred without manipulation of intracellular calcium levels, suggesting that S100 proteins perform important functions in cells at resting as well as increased intracellular calcium levels. Phenotypic changes in intact cells expressing altered levels of other members of the S100 family have also been observed without manipulation of intracellular calcium levels, including S100B (*5*, *6*), S100A4 or mts1 (*7*, *8*), and S100A6 or 42C (*9*).

Previous studies documenting increased S100A1 levels in renal cell carcinoma and melanoma (*10*, *11*) suggest that S100A1 may participate in the disease process. Other investigators (see ref *12*) have postulated that S100A1 contributes to the progression of diseases such as Alzheimer's disease in which changes in intracellular calcium levels have been documented and would result in changes in S100A1

† Supported by grants from the National Institutes of Health (NS 30660 to D.B.Z. and GM 52071 to D.J.W.), the Pine Family Foundation (D.B.Z.), and SRIS and DRIF funding from the State of Maryland.

* To whom correspondence should be addressed. Phone: 334-460-6794. Fax: 334-460-6798. E-mail: dzimmer@jaguar1.usouthal.edu.

‡ University of South Alabama.

§ University of Maryland School of Medicine.

10.1021/bi9817921 CCC: $15.00
Published on Web 11/26/1998

mediated signal transduction. Our previous studies documenting increased proliferation in S100A1 expressing neuronal cells (*4*) and increased susceptibility of S100A1 expressing neuronal cells to the neurotoxic Aβ peptide which is involved in Alzheimer's disease (*13*) confirm in intact cells that S100A1 can contribute to the increased proliferation of cancer cells as well as the neuronal cell death which occurs in Alzheimer's disease. While these previous studies suggest that S100A1 antagonists would be valuable adjunct therapy in the treatment of some diseases, there is no information available regarding the target proteins with which S100A1 interacts to regulate cell proliferation or Aβ-toxicity, nor have the molecular mechanisms of S100A1−target protein interactions been ascertained. Both of these pieces of information are essential for the rational design of S100A1 antagonists.

In vitro biochemical studies have identified many potential S100A1 target proteins, some exhibit modulation only in the presence of calcium (calcium dependent) and others exhibit modulation in the presence and absence of calcium (calcium independent) (see ref *1*). The list of calcium-dependent S100A1 target proteins includes twitchin kinase (*14*), the brain-specific aldolase C isoform (*15*), the transcription factor MyoD (*16*), and a dodecylpeptide (TRTK) of the actin-capping protein CapZ (*17*). The list of calcium-independent S100A1 target proteins includes the muscle-specific aldolase A isoform (*15*), glycogen phosphorylase a (*18*), phosphoglucomutase (*19*), and the Ca^{2+} release channel (ryanodine receptor) of skeletal muscle (*20*). Like other members of the calmodulin/troponin C/S100 superfamily of calcium receptor proteins (see ref *21*), S100A1 binds calcium via EF-hand calcium-binding motifs and undergoes a conformational change that exposes a hydrophobic patch (see ref *1*). This hydrophobic patch allows calcium receptor proteins, including S100A1, to interact with hydrophobic resins such as phenyl-Sepharose, a property which is utilized in the purification of these proteins. If the hydrophobic patch is a major contributor to interaction with calcium-dependent target proteins, then its unavailability in the absence of calcium suggests that calcium-independent target proteins will utilize a different mechanism to interact with S100A1.

While previous studies have implicated the carboxyl-terminus of S100 proteins in both calcium-dependent and calcium-independent target protein interactions, there is no direct evidence to support this hypotheis. In addition, the phenyl-Sepharose-binding region (PSBR)[1] which is exposed upon calcium-binding has not been identified nor has the relationship of the PSBR to the target protein binding site-(s) been established. In this study, point mutations and deletion mutations in the carboxyl-terminus of S100A1 have been used to identify residues involved in the interaction of S100A1 with calcium-dependent (the dodecylpeptide TRTK) and calcium-independent (Aldolase A) target proteins. First, a recombinant S100A1 protein (recS100A1) was expressed in bacteria, purified, and determined to exhibit physical properties which were indistinguishable from native S100A1. Next, proteins lacking the carboxyl-terminal nine residues of recS100A1 (Δ85−93), or containing alanine substitutions at Phe 88 (F88A), Phe 89 (F89A), or Trp 90 (W90A), both Phe 88 and Phe 89 (F88/89A), or all three aromatic residues (F88/89A−W90A) were recombinantly expressed. The inability of the Δ85−93 protein to interact with the calcium-dependent target TRTK and to bind phenyl-Sepharose demonstrates that the calcium-dependent target protein interaction domain and the PSBR are indistinguishable. However, the Δ85−93 protein did activate the calcium-independent target protein aldolase A, indicating that S100A1 utilizes different mechanisms to activate calcium-independent and calcium-dependent target proteins. Characterization of the single, double, and triple point mutations of the three hydrophobic residues in the carboxyl-terminus demonstrated that F88, F89, and W90 are major contributors to both the PBSR and the calcium-dependent target protein binding domain.

EXPERIMENTAL PROCEDURES

Cloning of RecS100A1. A rat kidney S100A1 cDNA (*22*) lacking the coding sequence for the 10 amino-terminal amino acids was ligated to synthetic oligonucleotides encoding the 10 amino-terminal amino acids of bovine S100A1. The resulting S100A1 coding sequence was ligated into the *Eco*RI−*Hin*dIII restriction sites of the pKK vector and the resulting plasmid (pKKA1) was used to transform competent UT481 *Escherichia coli* cells. T7 terminator primer (Novagen, Madison, WI), S100A1/*Nde*I primer (DNAgency, Aston, PA), and the pKKA1 template were used in mismatch PCR to create an *Nde*I restriction site at the translation initiation codon. Thirty cycles of PCR using Vent polymerase (New England Biolabs, Beverly, MA) were performed with each cycle consisting of 1 min, 94 °C; 1 min, 65 °C; 0.5 min, 72 °C. The PCR product was digested with *Nde*I and *Hin*dIII, ligated into *Nde*I- and *Hin*dIII-digested pET 21a(+) vector (Novagen), and the resulting construct was used to transform competent HMS174/DE3 *E. coli* cells. The presence of insert DNA was verified by *Spe*I restriction mapping. One clone was selected and the correct DNA coding sequence was verified using the *fmol* cycle sequencing protocol (Promega).

Cloning of Point Mutant S100A1 Proteins. A sense and antisense pair of exactly complementary oligonucleotides was synthesized (Gibco BRL, Gaithersburg, MD) for each point mutation. Point mutagenesis was performed using the QuikChange mutagenesis kit (Stratagene, La Jolla, CA) according to the manufacturer's protocol. One clone was selected for each mutation, and the entire DNA protein coding sequence was verified by cycle sequencing (Promega). These constructs were used to transform HMS174/DE3 *E. coli* cells.

Cloning of the Δ85−93 Mutant. T7 promoter (Novagen) and the Deletion 85−93 primer were used in PCR to delete amino acid residues 85−93 of recS100A1. The deletion 85−93 primer contained a stop codon and a *Hin*dIII restriction site. Vent polymerase was used in 30 cycles of PCR with each cycle consisting of 1 min, 94 °C; 1 min, 65 °C; and 0.3 min, 72 °C. The resulting PCR product was gel purified and restriction digested with *Nde*I and *Hin*dIII. The digested fragment was ligated into *Nde*I−*Hin*dIII-digested pET 21a-(+) vector and the resulting construct used to transform HMS174/DE3 *E. coli* cells. Potential clones were screened

[1] Abbreviations: BME, β-mercaptoethanol; DTT, dithiothreitol; DEAE, diethylaminoethyl-cellulose; EDTA, ethylenediaminetetraacetic acid; EGTA, [ethylenebis(oxyethylenenitrilo)]tetraacetic acid; IPTG, isopropyl thio-β-D-galactoside; MES, 2-[*N*-morpholino]ethanesulfonic acid; PAGE, polyacrylamide gel electrophoresis; PCR, polymerase chain reaction; PSBR, phenyl-Sepharose-binding region; SDS, sodium dodecyl sulfate; TRTK, dodecylpeptide derived from actin-binding protein CapZ.

by colony PCR using the T7 promoter and T7 terminator primers (Novagen) and Taq polymerase (Promega) under the following conditions: one cycle of 5 min, 95 °C; 1 min, 35 °C; 0.5 min, 95 °C; 30 cycles of 1 min, 94 °C; 1 min, 55 °C; 3 min, 72 °C; 7 min, 72 °C. The DNA protein coding sequence of one clone was confirmed by cycle sequencing (Promega).

Overexpression and Purification of Recombinant/Mutant S100A1 Proteins. Protein expression and bacterial lysis were performed as recommended by the manufacturer (Novagen). Bacterial lysates were boiled for 10 min and heat-labile proteins removed by centrifugation at 12000*g* for 10 min at 4 °C. Sodium chloride was added to the heat stable lysate fraction to a final concentration of 0.1 M, and the sample was loaded onto a DE52 diethylaminoethyl-cellulose (DEAE) column (Whatman, Inc., Fairfield, NJ). The column was equilibrated and unbound proteins eluted with three column volumes (~75 mL) of buffer A (20 mM Tris, pH 7.4, 1 mM EGTA, and 1 mM DTT) containing 0.1 M NaCl. S100A1 was eluted with buffer A containing 0.3 M NaCl and 30 1.5 mL fractions were collected. Fractions were analyzed by SDS−PAGE (*23*), and S100A1 protein-containing fractions were pooled. The column was washed between samples with buffer A containing 0.5 M NaCl.

Pooled DEAE column fractions were diluted with an equal volume of distilled water. $CaCl_2$ and Tris, pH 7.5, were added to a final concentration of 10 mM and 50 mM, respectively. The S100A1 protein-containing sample was applied to a phenyl-Sepharose column, and the column washed with three column volumes (~30 mL) of buffer B (5 mM $CaCl_2$, 1 mM DTT, and 50 mM Tris, pH 7.4), followed by buffer B containing 500 mM NaCl. S100A1 proteins (except Δ85−93) were eluted with buffer C (5 mM EDTA, 1 mM DTT, and 50 mM Tris, pH 7.4). The Δ85−93 protein was collected in the first 12 mL of buffer B wash, and this sample was applied to a second DEAE column which had been equilibrated with buffer A containing 0.1 M NaCl. The column was washed with 3 column volumes (~30 mL) of buffer A containing 0.1 M NaCl. The Δ85−93 protein was eluted from the column with 50 mM (MES) buffer, pH 4.5, containing 0.1 M NaCl. Fractions containing S100A1 proteins were identified by SDS−PAGE (*27*) and dialyzed extensively against distilled water in a 28-well microdialysis unit (Gibco BRL) equipped with 6000−8000 Da exclusion limit dialysis membrane.

Recovery of Recombinant/Mutant S100A1 Proteins after Boiling. Fifty microliters of 10 mg/mL aldolase protein was prepared from an ammonium sulfate suspension by centrifugation for 2 min in a microcentrifuge, followed by resuspension and dilution of the pellet in 50 mM Tris, pH 8.6, to a final protein concentration of 1.1 mg/mL. RecS100A1 and mutant proteins were each diluted to a concentration of 0.289 mg/mL. Aliquots of 10 μL were taken in duplicate for each protein and the protein content determined as described below. Fifty microliters of recS100A1, mutant proteins, and fructose-1,6-bisphosphate aldolase (Boehringer Mannheim) were each incubated in microcentrifuge tubes in a boiling water bath for 10 min. The samples were centrifuged for 20 min in a microcentrifuge at room temperature. The protein content of 10 μL of the supernatant was determined in duplicate as described below. The percent recovery was defined as the (micrograms of protein in 10 μL after boiling per microgram of protein in 10 μL before boiling) × 100.

Protein Chemistry. Amino acid composition analysis and amino terminal sequencing were performed at the University of Nebraska Protein Structure Core Facility (Omaha, NE). Purified recS100A1 and mutant proteins were prepared for amino acid composition analysis and recS100A1 was prepared for amino-terminal sequencing by aliquoting onto Prosorb membranes (Perkin-Elmer, Foster City, CA) using the protocol supplied by the company.

Nondenaturing Gel Electrophoresis. Nondenaturing gel electrophoresis was performed as previously described (*24*). Running buffer containing 10 mM $CaCl_2$ or 10 mM EDTA was used to generate the calcium-bound and the apo-proteins, respectively.

Gel Filtration Chromatography. A Superose 12 gel filtration column (Pharmacia Biotech, Piscataway, NJ) was used with an automated FPLC system (Pharmacia) at a flow rate of 0.3 mL/min. Proteins were extensively dialyzed against distilled water and filtered through a 0.22 μm syringe filter. The column was prerinsed with several volumes of buffer D (10 mM Tris, pH 7.4, 50 mM NaCl, 2 mM BME, and 2.5 mM $CaCl_2$) and calibrated using low molecular mass protein standards (Pharmacia). The protein standard mix included ribonuclease A (M_r 13.7 kDa), chymotrypsinogen A (M_r 25.0 kDa), ovalbumin (M_r 43.0 kDa), and bovine serum albumin (M_r 67.0 kDa) (50 μg each/mL; 200 μg of total protein/mL). The optical density of the eluate was measured at 280 nm wavelength. The K_{av} values were determined for ribonuclease A (M_r 13.7 kDa) and chymotrypsinogen A (M_r 25.0 kDa) using the equation $K_{av} = (V_e - V_o)/(V_t - V_o)$, where V_e is the elution volume at the peak apex, V_o is the void volume, and V_t is the total column volume. V_t and V_o were estimated as recommended by the manufacturer to be 24 and 8.4 mL, respectively. A standard curve was generated by plotting the K_{av} value versus the log of the molecular mass for ribonuclease A (M_r 13.7 kDa) and chymotrypsinogen A (M_r 25.0 kDa). Twelve micrograms of recS100A1 or 30 μg of mutant S100A1 protein was applied to the Superose 12 column. K_{av} values of the S100 proteins were determined using the equation above, and the molecular masses of the proteins were obtained using a standard curve of ribonuclease A and chymotrypsinogen A determined on the same day.

TRTK Tryptophan Fluorescence. Fluorescence data were collected using SLM-Aminco series 2 fluorescence spectrophotometers equipped with temperature controllers which maintained the temperature at 22 °C. Measurements were performed in a quartz cuvette with 0.2 and 1 cm excitation and emission path lengths, respectively. The excitation wavelength was 295 nm with a 4 nm slit width. The emission was scanned from 310 to 500 nm to determine the emission wavelength maximum for TRTK dodecylpeptide with a slit width of 8 nm. The binding of W90A and Δ85−93 proteins to TRTK peptide was monitored by an increase in fluorescence intensity at 332 nm during titrations of either W90A or Δ85−93 into a solution of TRTK peptide. All measurements were performed in 6 mM $CaCl_2$ and 25 mM Tris-HCl, pH 7.5, buffer. Data for these binding studies were fit to a single site binding model with one TRTK peptide bound per subunit protein. The changes in fluorescence at 332 nm ($I - I_o$) at different S100A1 concentrations were used to determine the dissociation (K_d) of the TRTK peptide from

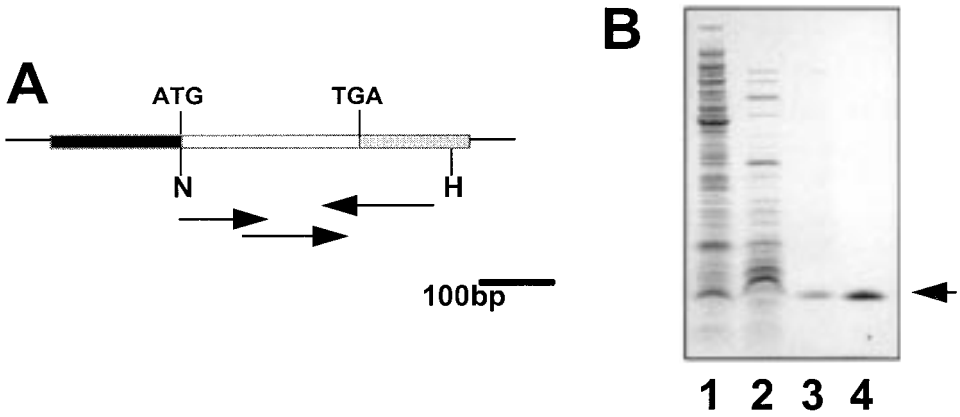

FIGURE 1: Purification and characterization of recS100A1. (A) Diagram of a portion of the S100A1 bacterial expression vector. Coding sequence is indicated in white rectangle, 3′ nontranslated sequence in the gray rectangle, the pET 21 vector *T7lac* promoter sequence in the black rectangle and portions of the pET vector backbone in the black lines. Arrows indicated the direction and extent of DNA sequence analysis. Also shown are the *Nde*I (N) and *Hin*dIII (H) restriction enzyme sites as well as the initiation (ATG) and stop (TGA) codons. (B) An IPTG- induced bacterial lysate (lane 1), DEAE flow-through (lane 2), and phenyl-Sepharose eluate (lane 3) of the recS100A1 and native S100A1 (lane 4) were size-fractionated on 10% SDS−polyacrylamide gels using a Tris-tricine buffer system (*27*). The arrow denotes the S100A1 band.

the S100A1−Ca-TRTK complex using the equation $I - I_o = (I_F - I_o[S100A1])/[S100A1] + K_d$ where I_o is the fluorescence prior to S100A1 addition, I is the fluroescence at varying S100A1 concentrations, and I_F is the fluroescence at saturating levels of peptide.

Aldolase Stimulation Assay. S100A1 stimulation of rabbit muscle aldolase (Aldolase A) (Boehringer Mannheim Corp., Indianapolis, IN) was determined as previously described (*15*). This method utilizes the colorimetric aldolase assay procedure no. 750 (Sigma Chemical Co.), which is based on the method of Sibley and Lehninger (*25*). Aldolase A stimulation is expressed as fold increase over baseline aldolase activity in the absence of recS100A1 (baseline = 1.0-fold). Stimulation of aldolase A activity by mutant S100A1 proteins was determined in the presence of 0.1, 1, 3, 5.8, and 10 μM mutant S100A1 protein. Each point represents the mean fold increase over basal activity of three determinations ± the standard error of the mean. The statistical significance ($p < 0.05$) of the data was determined using a one-way ANOVA test (Graph Pad Instat, Graph Pad Software, San Diego, CA).

Determination of Protein Concentrations. An S100A1 protein standard was quantiated by amino acid composition analysis as described above. Protein concentrations were determined by the method of Bradford (*26*) using both the S100A1 protein and bovine serum albumin as standards. In all assays, the S100A1 and bovine serum albumin standard curves were indistinguishable.

RESULTS

Expression, Purification, and Characterization of RecS100A1. To determine the importance of S100A1 carboxyl-terminal residues in S100A1−target protein interaction using mutagenesis, it was necessary to overexpress recombinant S100A1 protein. Since S100A1 is not posttranslationally modified, a bacterial overexpression system was chosen. Since the first 10 amino acids of the rat and bovine S100A1s are identical, the rat/bovine chimera DNA sequence encoded an S100A1 protein which was identical to the rat S100A1. DNA sequence analysis confirmed that the construct had the expected sequence, except for one base in the wobble position of the Gln 72 codon which was changed from a guanine to an adenine (Figure 1A). However, this mutation did not result in amino acid substitutions. While uninduced lystates contained no proteins that comigrated with S100A1, approximately 4 mg of S100A1 were purified from 500 mL of IPTG-induced cultures using a combination of boiling, DEAE anion-exchange chromatography, and calcium-dependent phenyl-Sepharose chromatography (Figure 1B). These results demonstrate that the recombinantly expressed protein has a net negative charge and exposes a hydrophobic phenyl-Sepharose binding region in the presence of calcium. Amino acid composition analysis (Table 1) and amino-terminal amino acid sequence analysis (MGSELETAMETL-INVFHAHS) confirmed that the recombinant protein was S100A1 (see ref *27*). Interestingly, the N-terminal methionine was retained on approximately two-thirds of the protein molecules and was proteolytically cleaved by the host bacteria on the remaining one-third of the molecules. As shown in Table 2, recS100A1, like native S100 proteins, was recovered in the soluble fraction after boiling (Table 2). Gel filtration chromatography of recS100A1 on a Superose 12 column demonstrated that recS100A1 protein migrates at a molecular mass of 20.8 kDa (Figure 2A). This molecular mass is almost identical to the expected molecular mass of 21 kDa for an S100A1 dimer and confirms that the recombinant protein dimerizes. Altogether, these results demonstrate that a recombinantly expressed rat S100A1 protein has physical and chemical properties which are indistinguishable from native S100A1. Furthermore, our inability to detect contaminating proteins by gel electrophoresis, amino acid composition analysis, amino acid sequence analysis, and gel filtration chromatography indicated that the recS100A1 protein was of high purity.

Expression, Purification, and Characterization of Δ85−93. A cDNA encoding a mutant S100A1 protein lacking the nine carboxyl-terminal residues was prepared by PCR and subcloned into a pET expression vector as described in the Experimental Procedures. DNA sequence analysis of the resulting clone verified the deletion and the absence of additional mutations (data not shown). The deletion mutant protein eluted from the DEAE column under the same

Table 1: Amino Acid Composition Analyses of RecS100A1 and Mutant S100A1 Proteins[a,b]

	wt (calculated)[c]	rec-S100A1	Δ85−93	F88A	F89A	W90A	F88/89A	F88A/89A−W90A
Met	2 or 3	2.6	2.7	3.1	3.2	3.0	3.1	3.1
Ile	2	1.8	2.5	2.0	1.9	2.0	2.0	2.0
Leu	11	10.4	10.0	11.0	11.1	11.3	11.5	11.5
Ser	6	5.7	***5.0***	6.1	6.0	6.0	5.1	6.0
Gly	5	5.0	7.5	5.4	5.1	5.1	5.2	5.1
Ala	7	6.7	7.2	***7.9***	***8.0***	***8.1***	***9.2***	***10.2***
Val	8	6.8	7.3	7.4	7.5	7.7	7.9	7.8
Arg	0	0.0	0.8	0.2	0.1	0.1	0.2	0.1
Lys	9	8.5	8.3	8.7	8.8	9.2	9.3	9.4
Asx	14	14.7	***10.8***	15.1	15.0	13.5	13.9	13.8
Glx	14	14.5	***13.1***	14.3	14.4	13.7	14.0	13.9
Tyr	1	0.9	1.2	1.1	1.1	1.1	1.1	1.1
Cys	1	0.4	***0.0***	1.2	1.3	1.8	1.9	1.5
Phe	6	5.5	***3.8***	***5.0***	***5.1***	6.1	***4.1***	***4.1***
Thr	4	4.0	4.1	4.1	4.1	3.9	4.0	4.0
His	2	1.9	1.9	1.9	2.0	1.9	1.9	1.9
Pro	0	0.0	0.5	0.2	0.1	0.0	0.0	0.0

[a] Values represent moles amino acid per mole protein. [b] Values for amino acids which were expected to differ from wild type are indicated in bold/italic type. [c] Song and Zimmer (*27*)

Table 2: Recovery of Recombinant and Mutant S100A1 Proteins after Boiling[a]

protein	protein before boiling (μg)	protein after boiling (μg)	percent recovery
recS100A1	4.23	4.20	99
Δ85−93	1.87	1.80	96
F88A	2.42	2.22	92
F89A	2.32	2.37	102
W90A	2.17	2.17	100
F88/89A	2.12	2.04	96
F88/89A−W90A	1.99	1.97	99
aldolase	7.55	0.00	0

[a] Percent recovery defined as (micrograms of protein in solution after boiling per micrograms of protein in solution before boiling) × 100.

conditions as recS100A1, indicating that deletion of the carboxyl-terminus, including Glu91, did not alter the ability of the protein to bind anion-exchange resins. The induced protein was then loaded onto a phenyl-Sepharose column, but unlike recS100A1, did not bind in the presence of 5 mM calcium (Figure 4) or 15 mM calcium (data not shown). The induced protein was collected from the first 12 mL of calcium buffer wash (see Experimental Procedures) and no other proteins were detected by SDS−PAGE analysis. However, nucleic acid contamination was present in the protein sample, and was removed by pH-dependent DEAE chromatography (data not shown). Amino acid composition analysis confirmed the identity of the induced protein as Δ85−93 (Table 1). The purified Δ85−93 was recovered in the soluble fraction after boiling (Table 2) and retained the ability to activate aldolase A after boiling. Furthermore, the Δ85−93 protein eluted from a Superose 12 gel filtration column as a 20.3 kDa protein (Figure 2B), indicating that deletion of the carboxyl-terminal nine amino acids does not alter the ability of S100A1 to dimerize. Thus, the Δ85−93 protein exhibited similar physical properties as recS100A1, with exception that it does not contain a calcium-dependent phenyl-Sepharose-binding region. Similar to recS100A1, contaminanting proteins were not detected in any analyses indicating that the Δ85−93 protein was of high purity.

Expression, Purification, and Characterization of Point Mutant S100A1s. To determine the importance of the aromatic residues Phe 88, Phe 89, and Trp 90 in S100A1−target protein interactions, site-directed mutagenesis was used to mutate Phe 88 to Ala (F88A), Phe 89 to Ala (F89A), Trp 90 to Ala (W90A), Phe 88 and Phe 89 to Ala (F88/89A), and Phe 88, Phe 89, and Trp 90 to Ala (F88/89A−W90A). DNA sequence analysis of the entire protein coding sequence confirmed the point mutations and verified that no other mutations were present (data not shown). The mutant proteins were purified from bacterial lysates, and amino acid composition analysis verified that the induced proteins were the appropriate S100A1 mutant proteins (Table 1). All of the point mutant S100A1s were recovered in the soluble fraction after boiling (Table 2), retained the ability to activate aldolase A after boiling, interacted with positively charged DEAE resin in 0.1 M NaCl and not 0.3 M NaCl, and eluted from gel filtration columns as dimers (21.2−21.7 kDa molecular masses) (data not shown). Once again, contaminanting proteins were not detected in any of the purified mutant S100A1 protein preparations, indicating that the mutant protein preparations were of high purity.

To determine if the aromatic residues contributed to the phenyl-Sepharose-binding region, the calcium-dependent hydrophobic interaction of the point mutant proteins with phenyl-Sepharose was analyzed. The F88A, F89A, and W90A proteins each bound phenyl-Sepharose in the presence of calcium and were eluted in the presence of calcium-chelating agent (EDTA) in a manner identical to recS100A1 (Figure 3). These results suggest that mutation of one of the three carboxyl-terminal aromatic residues does not affect the phenyl-Sepharose-binding region (PSBR) of recS100A1. While mutation of one aromatic residue did not significantly diminish the PSBR, simultaneous mutation of two residues, Phe 88 and Phe 89, did alter the PSBR. The F88/89A protein bound phenyl-Sepharose in the presence of calcium. However, a significant amount of protein was detected in the calcium buffer washes (Figure 3, lanes 4 and 5) and the F88/89A protein eluted in earlier fractions (Figure 3, compare lane 9 with lane 10) than the single point mutations (Figure 3, compare lanes 9 with lanes 10). These results indicate that mutation of the F88 and F89 to alanines weakens the interaction of S100A1 with phenyl-Sepharose and that F88 and F89 contribute to the PSBR. While some of the triple point mutant F88/89A−W90As bound phenyl-Sepharose in

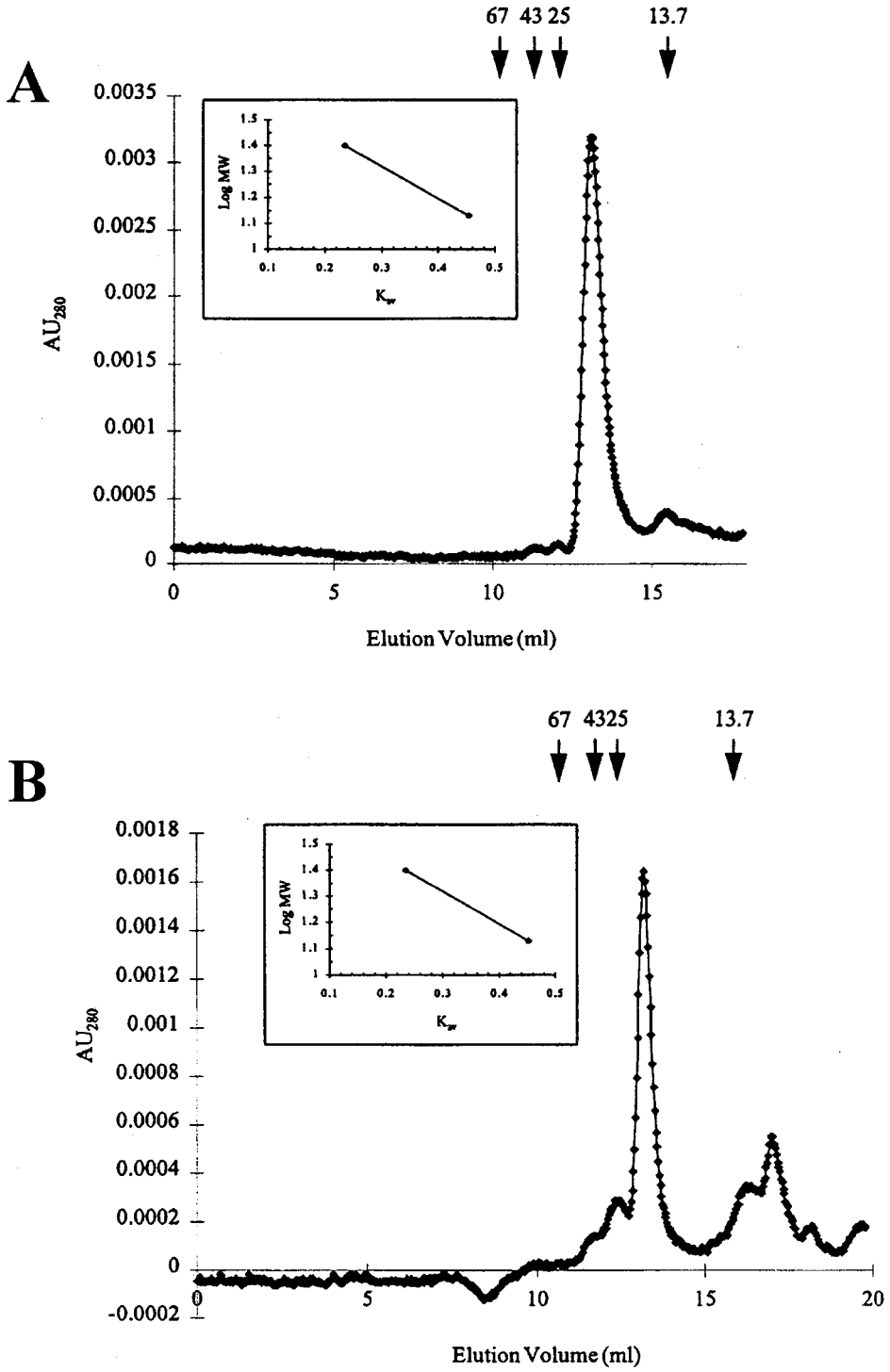

FIGURE 2: Gel filtration chromatography of recS100A1 and mutant S100A1s. (A) Chromatogram of approximately 12 μg of recS100A1 fractionated on a Superose 12 gel filtration column. (B) Chromatogram of approximately 30 μg of D85−93 protein fractionated on a Superose 12 gel filtration column. Arrows indicate the elution volumes for the 13.7, 25, 43, and 67 kDa molecular mass standards. Insets show the standard curve generated by plotting the K_{av} value against the log molecular mass of the 13.7 and 25 kDa standard proteins.

the presence of calcium, some of the F88/89A−W90A protein was detected in the column flow-through (Figure 3, lane 3), a significant amount of protein was present in the calcium buffer washes (Figure 3, lanes 4 and 5), and the bound protein eluted from the column in earlier fractions than recS100A1. These results suggest that all three carboxyl-terminal aromatic residues contribute to the PSBR.

Nondenaturing Gel Electrophoresis of RecS100A1 and Mutant S100A1 Proteins. In the presence of calcium, the migration of calcium-binding proteins such as calmodulin and S100 proteins on tris-glycine gels containing no SDS is shifted to the cathode (see ref *24*). This change in migration is due to the change in net negative charge which occurs upon calcium binding. Nondenaturing gel electrophoresis was used in this study to determine if the mutations caused any alterations in S100A1 calcium binding. All point mutant and deletion mutant S100A1 proteins exhibited shifts in migration similar to recS100A1 in the presence of saturating calcium levels (10 mM $CaCl_2$) (Figure 4). These results indicate that deletion of residues 85−93 or point mutation of the three

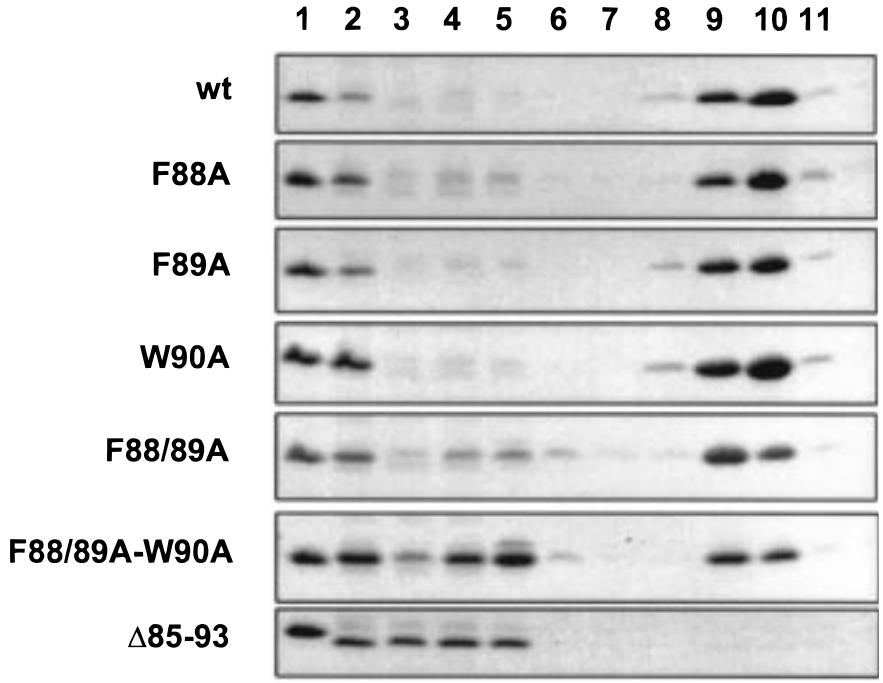

FIGURE 3: Phenyl-Sepharose chromatography of native, recombinant, and mutant S100A1s. Standardized phenyl-Sepharase columns of equivalent size and volume as well as fraction size were used to chromatogram equivalent volumes and quantities of recombinant and mutant S100A1 proteins. The fractions which were loaded on the phenyl-Sepharose column are shown in lane 2. The unbound protein fraction is shown in lane 3, the calcium-containing buffer fractions in lanes 4 and 5, the salt and calcium-containing buffer fractions in lanes 6 and 7, and the EDTA containing fractions in lanes 8−11. Lane 1 contains purified recS100A1.

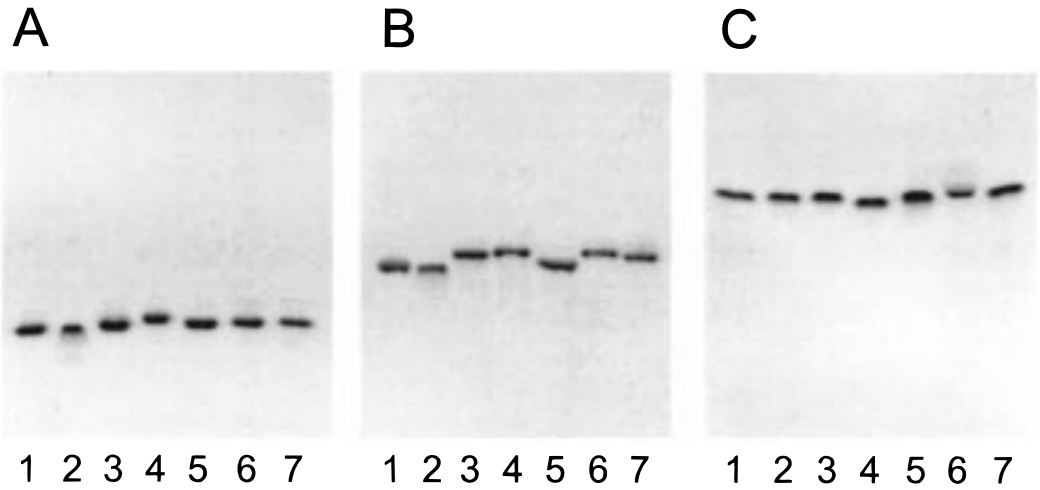

FIGURE 4: Nondenaturing gel electrophoresis of recombinant and mutant S100A1s. Three micrograms of recS100A1 (lane 1), D85−93 (lane 2), F89A (lane 3), F88A (lane 4), W90A (lane 5), F88/89A (lane 6), and F88/89A−W90A (lane 7) were electrophoresed on 15% nondenaturing gels in the presence of 5 mM EDTA (panel A), 0.01 mM $CaCl_2$ (panel B), or 5 mM $CaCl_2$ (panel C) from the anode (top) to the cathode (bottom). Proteins were visualized by Coomassie Blue staining.

carboxyl-terminal aromatic residues does not alter the ability of S100A1 to bind calcium at millimolar concentrations. Thus, the decreased binding of these mutants to phenyl-Sepharose is not due to decreased calcium binding but to alterations in the hydrophobic patch. Furthermore, in the presence of four different concentrations of $CaCl_2$ (0, 0.01, 0.1, and 5 mM), all proteins exhibited identical shifts in migration. In the presence of subsaturating calcium concentrations, the shift observed was intermediate between that observed in the absence or presence of saturating calcium levels (Figure 4), suggesting that binding of calcium to the carboxyl-terminal cannonical EF-hand in S100A1 is not altered by the point mutations or the deletion mutation.

Calcium-Dependent TRTK Binding. S100A1 interaction with dodecylpeptide TRTK was monitored by measuring fluorescence of the single tryptophan in the TRTK peptide (TRTKIDWNKILS). Upon addition of the W90A mutant into TRTK peptide, a 20 nm blue shift of fluorescence maxima was observed (from 352 to 332 nm), whereas a 4−5 nm blue shift was observed for Δ85−93 mutant (Figure 5A). The larger blue shift observed for the W90A mutant (20 nm) versus the Δ85−93 mutant (4 nm) is consistent with the loss of hydrophobic interactions between the Δ85−93 mutant and the TRTK peptide. Titration curves illustrating the binding of the W90A and Δ85−93 mutant proteins to the TRTK peptide clearly show that the Δ85−93 mutant (K_d of >30

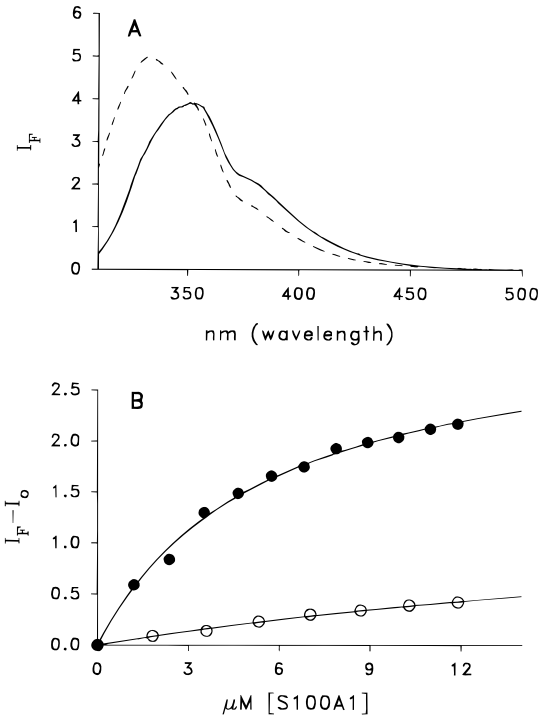

FIGURE 5: Ca^{2+}-dependent binding of the dodecylpeptide TRTK binding to recombinant and mutant S100A1s. (A) Flourescence spectra of the TRTK peptide in the absence (solid line) and presence (dashed line) of S100A1 were scanned from 310 to 500 nm with a 295 nm excitation wavelength. (B) Fluorescence titrations of the TRTK peptide with W90A S100A1 (filled circles) or D85−93 S100A1 (open circles) were monitored by the increase of emission at $\lambda = 338$ nm and plotted as a function of S100A1 concentration. The dissociation (K_d) of the TRTK peptide from the S100A1-Ca-TRTK complex was determined using the equation $I - I_o = (I_F - I_o[S100A1])/[S100A1] + K_d$ where I_o is the fluorescence prior to S100A1 addition, I is the fluroescence at varying S100A1 concentrations, and I_F is the fluroescence at saturating levels of peptide. The D85−93 mutant had a lower affinity ($K_d > 30$ mM) for the dodecylpeptide that the W90A mutant ($K_d = 5.55$ mM). In both panels A and B, the solutions contained 7.5 μM TRTK peptide, 6 mM $CaCl_2$, and 12.5 mM Tris buffer, pH 7.5, 22 °C.

μM) has a lower affinity for the peptide than the W90A mutant (K_d of 5.55 μM) (Figure 5B). In the absence of Ca^{2+}, no change in TRTK peptide fluorescence was observed upon the addition of W90A or Δ85−93 mutant proteins. Together, these results indicate that residues in the C-terminus of S100A1 (residues 85−93) contribute significantly to the calcium-dependent binding of S100A1 to TRTK peptide.

Calcium-Independent Stimulation of Aldolase A Activity. To determine the role of carboxyl-terminal residues of S100A1 in S100A1−target protein interaction, the effects of each mutant protein on aldolase A activity was assessed. Each mutant S100A1 protein or recS100A1 was added to the aldolase A assay to a final concentration of 0.1, 1, 3, 5.8, or 10 μM. At each concentration, mutant protein stimulation of aldolase A activity was not statistically significantly different ($p < 0.05$) from recS100A1 (Figure 6). All mutant proteins maximally stimulated aldolase A to approximately 2.0-fold over baseline activity, which is comparable to the 1.8-fold stimulation by native S100A1 and S100B observed by Zimmer and Van Eldik (*15*). As previously reported for native S100A1 (*15*), stimulation of aldolase A activity by all mutant proteins was calcium independent and occurred in the presence and absence of

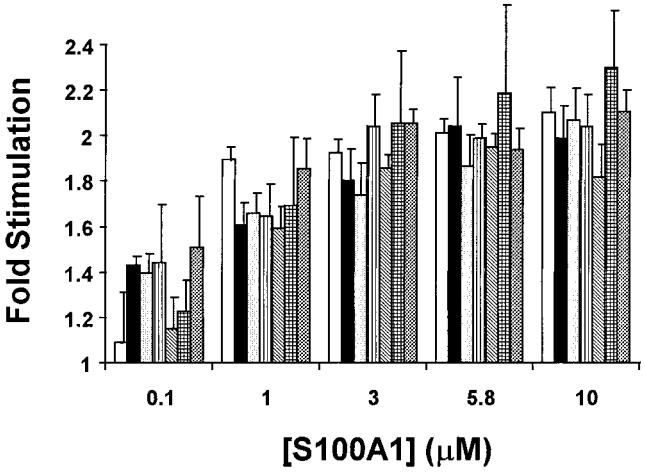

FIGURE 6: Stimulation of aldolase A activity by recombinant and mutant S100A1s. Aldolase activity was determined in the presence of increasing concentrations of recS100A1 (white bars), F88A (black bars), F89A (dotted bars), W90A (vertically stripped bars), F88/89A (hatched bars), F88/89A−W90A (checked bars), or D85−93 (gray bars) and 1 mM $CaCl_2$. Basal aldolase activity observed in the absence of S100A1 protein was normalized to 1.0 and the activity observed in the presence of S100 expressed as the mean fold stimulation ± the standard error of the mean. For recS100A1 n (number of determinations) = 2−20 and for all mutant S100A1s, $n = 3$.

calcium. These results demonstrate that the aromatic residues Phe 88−Trp 90 or other residues in the carboxyl-terminus are not necessary for the calcium-independent interaction of S100A1 with aldolase A.

DISCUSSION

The present study examines the role of carboxyl-terminal S100A1 residues in calcium-dependent interaction with phenyl-Sepharose and the target protein TRTK as well as calcium-independent interaction with the target protein aldolase A. Deletion of residues 85−93, the carboxyl terminal nine amino acids, altered calcium-dependent interaction with phenyl-Sepharose and the TRTK dodecylpeptide. In contrast, none of the mutants altered calcium-independent stimulation of aldolase A activity. Altogether, these data demonstrate that carboxyl-terminal residues comprise the phenyl-Sepharose-binding region of S100A1, designated PSBR, as well as the calcium-dependent target protein binding site. While residues in the PSBR have been hypothesized to participate in the interaction of calcium receptor proteins with calcium-dependent target proteins, this study presents the first direct evidence supporting that hypothesis.

There are three hydrophobic residues (Phe 88, Phe 89, and Trp 90) in the carboxyl-terminus of S100A1 which could comprise the PSBR. When alanines were substituted for all three aromatic residues (F88/89A−W90A), the protein exhibited calcium-dependent interaction with phenyl-Sepharose which was weaker than the F88/89A protein. Mutation of single aromatic residues to alanines did not alter phenyl-Sepharose binding. These data indicate that a combination of these aromatic residues comprise the PSBR. The residual calcium-dependent interaction of the F88/89A and F88/89A−W90A proteins with phenyl-Sepharose may be due to the hydrophobicity of the alanines which were used to substitute the aromatic residues. An alternative interpretation is that

residues other than the three hydrophobic residues contribute to the PSBR. These data are consistent with studies on other S100 proteins. Structural studies have implicated the carboxyl-terminus of S100B in interaction with two calcium-dependent target proteins: peptides of the tumor suppressor p53 (*28*, *29*) and TRTK and a peptide encoding a region of the actin capping protein CapZ (*30*). Although the carboxyl-terminal tail in S100A1 is one residue longer than that of S100B, there are four residues which are identical: Ala 84, Cys 85, Phe 88, and Phe 89. Kube and co-workers (*31*) demonstrated that carboxyl-terminal residues, particularly hydrophobic residues Tyr 85 and Phe 86, are necessary for the calcium-independent interaction of S100A10 with its target protein annexin II. S100A1 has analogous carboxyl-terminal aromatic Phe residues at positions 88 and 89 and an additional Trp at position 90. However, S100A10 does not bind calcium and has no calcium-dependent target proteins.

While the carboxyl-terminal amino acids of S100A1 are essential for interaction of S100A1 with calcium-dependent target proteins, they are not necessary for the calcium-independent interaction of S100A1 with aldolase A. This conclusion is supported by data in this study which demonstrates the stimulation of aldolase A activity by all mutant proteins to the same extent as recS100A1. Although there is no direct evidence demonstrating the types of interactions that may be involved in S100A1 interaction with calcium-independent target proteins, there is indirect evidence which suggests that ionic interactions may be involved. First, we have observed stimulation of aldolase A activity by nucleic acids. S100A1 has an isoelectric point of ~4.0 and, like DNA, is highly negatively charged at physiological pH. These properties are consistent with an ionic mechanism of interaction for S100A1 and aldolase. Second, Fujii and co-workers (*32*) reported that S100 protein binding to tubulin and tau proteins occurs in the absence of calcium and that the proteins can be dissociated by increasing ionic strength. These investigators propose that S100 binding to microtubule proteins is mediated by ionic interactions. Determination of the exact mechanism of interaction of S100 proteins with calcium-independent target proteins will require additional experimentation. Nonetheless, we do know that the mechanism of S100A1 interaction with its calcium-independent target protein aldolase A is not mediated by the analogous hydrophobic residues that mediate interaction of S100A10 with its calcium-independent target protein annexin (*31*). These data suggest that S100 proteins will utilize multiple mechanisms for interacting with target proteins and that some mechanisms may be utilized by some members of the family while other family members use different mechanisms. It will be important in future studies to identify and compare the target proteins as well as mechanisms of target protein interaction for various members of the S100 protein family.

Our current model for S100A1−target protein interactions is shown in Figure 7 and contains two distinct target protein binding regions. The first region is a calcium-dependent hydrophobic region. The PSBR, which consists of a cluster of three aromatic residues (F88−W90), is part of this calcium-dependent hydrophobic-binding site. The second site is a calcium-independent target protein binding site. Because previous studies have shown that calmodulin-target protein interactions vary from target protein to target protein (see ref *33*), the specific residues involved in the interactions diagramed in Figure 7 may vary from target protein to target protein. In the case of S100A1, it will be feasible to design agents that selectively interfere with S100A1 modulation of both calcium-dependent and calcium-independent interactions since the binding sites for these two classes of proteins are distinct.

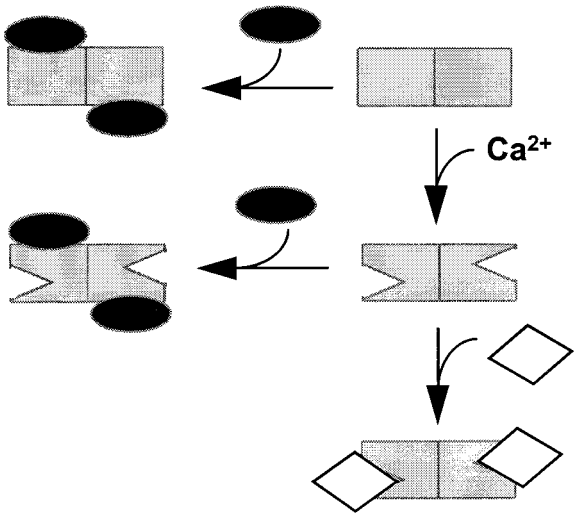

FIGURE 7: Model of S100A1−target protein interactions. The gray squares represent the S100A1 dimer, the black ellipses represent calcium-independent target proteins and the gray diamonds represent calcium-dependent target proteins.

REFERENCES

1. Zimmer, D. B., Cornwall, E. H., Landar, A., and Song, W. (1995) *Brain Res. Bull. 37*, 417−429.
2. Moore, B. (1965) *Biochem. Biophys. Res. Commun. 19*, 739−744.
3. Schafer, B. W., Wicki, R., Engelkamp, D., Mattei, M.-G., and Heizmann, C. W. (1995) *Genomics 25*, 638−643.
4. Zimmer, D. B., Cornwall, E. H., Reynolds, P. D., and Donald, C. M. (1998) *J. Biol. Chem. 273*, 4705−4711.
5. Scotto, C., Delloulme, J. C., Rousseau, D., Chambaz, E., Baudier, J. (1998) *Mol. Cell. Biol. 18*, 4272−4281.
6. Selinefruend, R. H., Barger, S. W., Welsh, J. J., and Van Eldik, L. J. (1990) *J. Cell Biol 111*, 2021−2028.
7. Lakshmi, M. S., Parker, C., and Sherbet, G. V. (1993) *Anticancer Res. 13*, 299−304.
8. Takenaga, K., Nakamura, Y., and Sakiyama, S. (1997) *Oncogene 14*, 331−337.
9. Masiakowski, P., and Shooter, E. M. (1990) *J. Neurosci. Res. 27*, 264−269.
10. Kato, K., Haimoto, H., Ariyoshi, Y., Horisawa, M., Washida, H., and Kimura, S. (1985) *Jpn. J. Cancer Res. 76*, 856−862.
11. Morii, K., Tanaka, R., Takahashi, Y., and Kuwano, R. (1992) *J. Neuro. Res. 32*, 27−33.
12. Schafer, B. W., and Heizmann, C. W. (1996) *Trends Biochem. Sci. 21*, 134−140.
13. Zimmer, D. B. (1997) *Soc. Neurosci. Abstr. 23*, 840.
14. Heierhorst, J., Kobe, B., Feil, S. C., Parker, M. W., Benian, G. M., Weiss, K. R., and Kemp, B. E. (1996) *Nature 380*, 636−639.
15. Zimmer, D. B., and Van Eldik, L. J. (1986) *J. Biol. Chem. 261*, 11424−11428.
16. Baudier, J., Bergeret, E., Bertacchi, N., Weintraub, H., Gagnon, J., and Garin, J. (1995) *Biochem. 34*, 7834−7846.
17. Ivanenkov, V. V., Dimlich, R. V., and Jamieson, G. A. Jr. (1996) *Biochem. Biophys. Res. Commun. 221*, 46−50.
18. Zimmer, D. B., and Dubuisson, J. G. (1993) *Cell Calcium 14*, 323−332.

19. Landar, A., Caddell, G., Chessher, J., and Zimmer, D. B. (1996) Identification of an S100A1/S100B target protein; phosphoglucomutase. *Cell Calcium 20*, 279−285.
20. Treves, S., Scutari, E., Robert, M., Groh, S., Ottolia, M., Prestipino, G., Ronjat, M., and Zorzato, F. (1997) *Biochemistry 36*, 11496−11503.
21. Smith, V. L., Kaetzel, M. A., and Dedman, J. R. (1990) *Cell Regul. 1*, 165−172.
22. Zimmer, D. B., Song, W., and Zimmer, W. E. (1991) *Brain Res. Bull. 27*, 157−162.
23. Schagger, H., and von Jagow, G. (1987) *Anal. Biochem. 166*, 368−379.
24. Landar, A., Hall, T. L., Cornwall, E. H., Correia, J. J., Drohat, A. C., Weber, D. J., and Zimmer, D. B. (1997) *Biochim. Biophys. Acta 1343*, 117−129.
25. Sibley, J. A., and Lehninger, A. L. (1949) *J. Biol. Chem. 177*, 859−872.
26. Bradford M. M. (1976) *Anal. Biochem. 72*, 248−254.
27. Song, W. E., and Zimmer, D. B. (1996) *Brain Res. 721*, 204−216.
28. Rustandi, R., Drohat, A. C., Baldiserri, D. M., Wilder, P. T., and Weber, D. J. (1998) *Biochemistry 37*, 1951−1960.
29. Wilder, P. T., Rustandi, R. R., Drohat, A. C., and Weber, D. J. (1998) *Protein Sci. 7*, 794−798.
30. Kilby, P. M., Van Eldik, L. J., and Roberts, G. C. (1997) *Protein Sci. 6*, 2494−2503.
31. Kube, E., Becker, T., Weber, K., and Gerke, V. (1992) *J. Biol. Chem. 267*, 14175−14182.
32. Fujii, T., Gocho, N., Akabane, Y., Kondo, Y., Suzuki, T., and Ohki, K. (1986) *Chem. Pharm. Bull. 34*, 2261−2264.
33. Weber, P. C., Lukas, T. J., Craig, T. A., Wilson, E., King, M. M, Kwiatkowski, A. P., and Watterson, D. M. (1989) *Protein Struct., Funct., Genet. 6*, 70−85.

BI9817921